Binary Iron−Dinitrogen Compounds Synthesized by Co-deposition of Mass-Selected Fe, Fe₂, and Fe₃ with N₂

T. L. Haslett,*,† S. Fedrigo,† K. Bosnick,† M. Moskovits,† H. A. Duarte,‖,‡ and D. Salahub‖,§

*Contribution from the Department of Chemistry, University of Toronto, 80 St. George St.,
Toronto, Ontario M5S 3H6, Canada, Département de Chimie, Université de Montréal, C.P. 6128,
Succursale centre-ville, Montréal, Québec H3C 3J7, Canada*

Received November 4, 1999

Abstract: Iron−nitrogen binary complexes were synthesized by co-depositing mass-selected Fe^+, Fe_2^+, and Fe_3^+ with N_2 and electrons to form a matrix. The resulting compounds were observed using FTIR spectroscopy. The trigonal-bipyramidal $Fe(N_2)_5$ structure assigned from the spectra of the Fe^+ deposits is supported by density functional calculations involving full geometry optimizations with all symmetry conditions relaxed for $Fe(N_2)_x$ ($x = 1$ to 5) binary compounds. FTIR spectra of $Fe_2(N_2)_x$ and $Fe_3(N_2)_y$ are also reported. Structures for the dimer and trimer dinitrogen complexes have not been deduced since the spectra are too weak to perform isotopic substitution experiments.

Introduction

The interaction between Fe clusters and N_2 is of great interest in the widely different fields of catalysis, biology, and cluster science. In catalysis, it is the dissociation of N_2 over Fe in the Haber process that is critical in the production of NH_3,[1] while the fixation of nitrogen by the nitrogenase enzyme is the equivalent process in biological systems.[2] Although N_2 is often thought of as highly inert, these reactions with transition metals and/or their complexes demonstrate that breaking the N−N triple bond can be relatively facile under the right conditions. Metal cluster research has demonstrated that reactions involving metals can be highly dependent on the cluster size.[3] The behavior of dinitrogen reacting with iron clusters of different nuclearity is therefore particularly relevant to industrial and biological processes involving N−N bond breaking.

Because of the catalytic importance, a considerable amount of work has been done on N_2 physisorbed and chemisorbed on Fe surfaces.[4] Despite the interest in this class of reactions, surprisingly little is known about how nitrogen reacts with iron atoms and clusters. In early experiments involving iron atoms co-deposited with Ar or N_2 in low-temperature matrices, Mössbauer, UV−visible, and IR spectra indicated that Fe atoms do not react with N_2 while Fe_2 and possibly Fe_3 react to form binary complexes.[5,6] Furthermore, the IR spectrum assigned to the Fe_2/N_2 reaction product was somewhat complicated, sug-

gesting either a number of different complexes gave rise to the spectrum or the product was a highly unsymmetric complex (at least in the matrix environment).[5] A similar experiment using lower Fe concentrations as well as mixed Ar/N_2 matrices showed that the IR spectrum initially reported was at least partly due to atomic species, tentatively assigned as $Fe(N_2)_5$.[7]

In a study of the IR spectra of a series of N_2 matrices with increasing Fe density, Bier and Moskovits[8] observed a smooth progression from the previously reported atomic spectrum[7] (peaks at 2016 and 2111 cm⁻¹) to the initially reported spectrum,[5] confirming its assignment to both Fe and Fe_2 dinitrogen species (Figure 1).[5] More recently, Mascetti and Elustando attributed FTIR spectra of iron in N_2 matrices almost entirely to Fe_2 and Fe_3 dinitrogen complexes.[9] While the spectra bear a resemblance to Figure 1C and ref 5, because of the much higher metal concentrations used, very little contribution from atomic species was observed. In the same work, a number of unsaturated atomic $Fe(N_2)_x$ and $Fe_2(N_2)_y$ species are assigned from relatively concentrated iron deposits in mixed Ar/N_2 matrices.

Using a different technique from thermal metal deposition, Andrews and co-workers have studied reactions of Fe atoms with N_2.[10] Fe metal was laser ablated and co-deposited with N_2 or an Ar/N_2 mixture on a cooled CsI window. Ablation yields hot atoms and ions, which are responsible for the observation of numerous products not observed in deposits produced from thermal evaporation Fe sources. Features in the IR spectrum were assigned to species FeN, NFeN, Fe_2N, $(Fe_2)(N_2)$, side-on

* Address correspondence to this author.
† University of Toronto.
‖ Université de Montréal.
‡ Present address: Laboratorio de Quimica Computacional e Modelagem Molecular, Departamento de Quimica, Universidade Federal de Minas Gerais, Av. Antonio Carlos, 6627, 31.270-901 − Belo Horizonte − MG, Brasil.
§ Present address: Steacie Institute for Molecular Sciences, National Research Council of Canada, 100 Sussex Dr., Ottawa, Ontario, Canada K1A 0R6.
(1) See for example: Ertl, G. *J. Vac. Sci. Technol. A* **1983**, *1*, 1247.
(2) *2) A Treatise on Dinitrogen Fixation*: *Sections 1 and 2*; Hardy, R. W., Bottomley, F., Burns, R. C., Eds.; Wiley: New York, 1979.
(3) Cluster reactivities vs size.
(4) Rao, C. N. R.; Ranga Rao, G. *Surf. Sci. Rep.* **1991**, *13*, 221.
(5) Barrett, P. H.; Montano, P. A. *J. Chem. Soc.*, *Faraday Trans. 2* **1977**, *73*, 378.

(6) Hulse, J. E. Ph.D. Thesis (University Microfilms, Ann Arbor, MI), University of Toronto, 1978: Moskovits, M. *Acc. Chem. Res.* **1979**, *12*, 229.
(7) Doeff, M. M.; Parker, S. F.; Barrett, P. H.; Pearson, R. G. *Inorg. Chem.* **1984**, *23*, 4108.
(8) Bier, K. D.; Moskovits, M. Unpublished work.
(9) Mascetti, J.; Elustondo, F. Private communication. Elustando, F. Ph.D. Thesis, L'Université Bordeaux I, 1998.
(10) Chertihin, G. V.; Andrews, L.; Neurock, M. *J. Phys. Chem.* **1996**, *100*, 14609. Andrews, L.; Chertihin, G. V.; Lanzisera, D. V. In *Proceedings of the 2nd International Conference on Low-Temperature Chemistry, Aug 4−9, 1996, Kansas City*; Durig, J. R., Klabunde, K. J., Eds.; Bookmark Press: Kansas City, 1996.
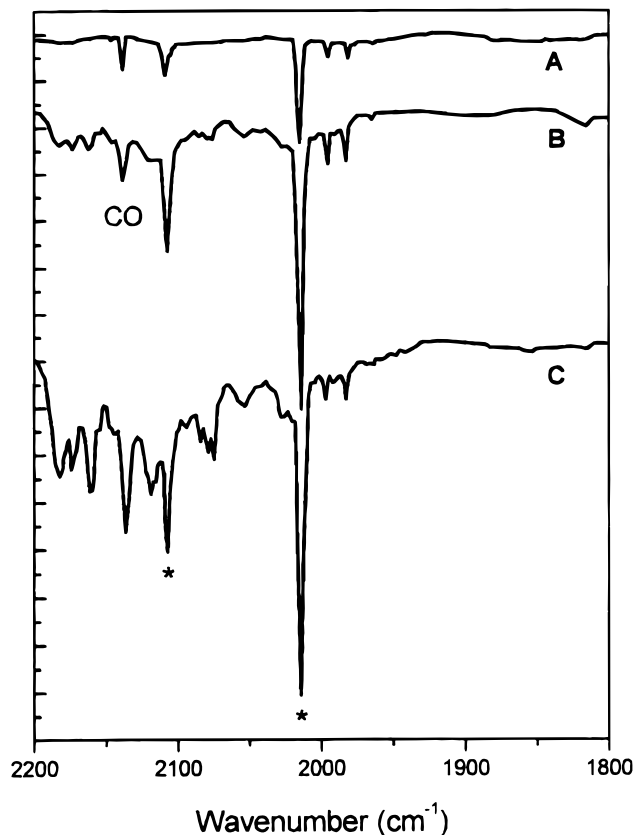
Figure 1. FTIR spectra of Fe in an N_2 matrix as a function of iron concentration: (A) 0.003%; (B) 0.006%; (C) 0.01%.[8] Peaks marked with an asterisk are assigned to $Fe(N_2)_y$ complexes, with all other peaks being assigned to $Fe_2(N_2)_y$ complex(es). The peak due to CO impurity is labeled.

and end-on $Fe(N_2)$, and $Fe(N_2)_x$. Interestingly, none of the peaks assigned to Fe/N_2 complexes in pure N_2 matrices by Andrews agree with the spectrum of the atomic complex observed in evaporated metal matrix deposits (Figure 1A and ref 7), suggesting that there are at least two stable $Fe(N_2)_x$ species in N_2 matrices, depending on the path of formation, and there is a nonnegligible barrier to saturation of the complex at matrix temperatures.

In this paper, we present the FTIR spectra of Fe/N_2 complexes formed by co-depositing mass-selected Fe^+, Fe_2^+, and Fe_3^+ with N_2 and electrons. Each deposit yielded a distinct and characteristic vibrational spectrum. Density functional theory calculations coupled with isotopic experiments on the Fe/N_2 system show that the atomic iron complex is the trigonal-bipyramidal $Fe(N_2)_5$, analogous to the isoelectronic $Fe(CO)_5$.

Experimental Section

The mass-selected cluster apparatus has been described previously.[11] Iron cluster ions were produced by high-voltage sputtering an Fe target (Aldrich 99.9%), mass-selected using a Wien filter, and co-deposited with N_2 (Matheson, 99.9999%) on a cold (20 K) cesium iodide window. Ions were neutralized with a low-energy electron beam situated 1 mm in front of the substrate. It is unclear whether the neutralization takes place before, during, or after the cluster-N_2 reaction; however, pressure, current, and mean-free-path considerations suggest that most likely the cluster ions undergo collisions with N_2 before being neutralized. The pressure in the deposition chamber was 6×10^{-10} Torr with the sample cold, rising to 8×10^{-10} Torr when the cluster beam is operating but

before N_2 is being injected. The pressure rise is almost entirely due to Ar from the sputter gun used in the ion source. The cluster ion currents used in the depositions were 16, 5, and 1 nA, respectively for Fe^+, Fe_2^+, and Fe_3^+, as measured on a 2 mm diameter Faraday plate. All cluster beams were deposited with a nominal kinetic energy of 20 eV and a beam diameter of approximately 3 mm full width at half-maximum. The deposition rate of N_2 was adjusted using a leak valve to obtain a N_2:cluster ratio of 10^4:1 in the matrix. Infrared absorption spectra were collected by passing the modulated beam of a 1 cm^{-1} resolution Fourier transform infrared spectrometer (Bomem MB100) through the sample and onto an MCT detector. The infrared beam was focused at the sample using a 35 cm focal length mirror external to the vacuum chamber. By passing the beam through a 2 mm high slit situated 4 mm in front of the sample and vertically translating the sample, the absorption could be measured as a function of the vertical position across the deposit. Peaks whose intensities correlated with the cluster beam profile were assumed to be related to species originating in the beam.

DFT Computational Details

$Fe(N_2)_x$ ($x = 1-5$) complexes were investigated using the LCGTO-KS-DF (Linear Combination of Gaussian Type Orbitals-Kohn Sham-Density Functional) method implemented in the program deMon-KS.[12] A brief description of some of the results follows. A more detailed report has been published elsewhere.[13] The generalized gradient approximation for the exchange and correlation (XC) functional has been used with the Becke[14] expression for exchange and that of Perdew[15] for correlation (GGA-BP). The basis set used has a contraction pattern for Fe of (63321/5211*/41+) and for N of (7111/411/1*), obtained as previously described.[16] Auxiliary basis sets used to fit the charge density (CD) and XC potentials had patterns of (5,5;5,5) and (4,3;4,3) respectively for Fe and N. In this notation ($k_1,k_2;l_1,l_2$), k_1 (l_1) is the number of s-type Gaussians in the CD (XC) basis and k_2 (l_2) is the number of s-, p-, and d-type Gaussians constrained to have the same exponent in the CD (XC) basis. The charge density was fit analytically while the XC potential was fit numerically using a grid of 48 radial shells and 26 angular points per shell, for a total of 1248 points per atom. The geometries were fully optimized without symmetry constraint by means of the Broyden−Fletcher−Goldfarb−Shanno (BFGS) algorithm,[17] leading to geometries slightly distorted from ideal due to numerical noise. Although the computational noise could be minimized by employing a finer grid of points, this more expensive calculation was not performed since the matrix environment of the $Fe(N_2)_x$ complexes in the experimental work is less homogeneous than the computational grid employed. The distorting effects of the matrix environment are well-known, for example, in the case of $Fe(CO)_5$ isolated in CO matrices.[11]

The optimized geometries of the complexes $Fe(N_2)_x$ ($x = 2-5$) are shown in Figure 2. All the N_2 ligands are end-bound in the lowest energy geometries, with the exception that for complexes with $x = 1$ and 2 there are geometries involving side-bound N_2 that are almost isoenergetic with the end-bound complex. An important distinction between the end- and side-bound species is that the N_2 vibrational frequency is calculated to be on the order of 200 cm^{-1} lower for the side-bound ligand, in good agreement with calculations and observations reported by Chertihin et al.[10] Table 1 summarizes the total energies and ligand binding energies of the lowest energy $Fe(N_2)_x$ complexes

(11) Fedrigo, S.; Haslett, T. L.; Moskovits, M. *J. Am. Chem. Soc.* **1996**, *118*, 5083.

(12) (a) Casida, M. E.; Daul, C.; Goursot, A.; Koester, A.; Pettersson, L.; Proynov, E.; St.-Amant, A.; Salahub, D. R.; Duarte, H. A.; Godbout, N.; Guan, J.; Jamorski, C.; Leboeuf, M.; Malkin, V.; Malkina, O.; Sim, F.; Vela, A. deMon Software-deMon-KS3 Module, Université de Montréal, 1996. (b) St. Amant, A.; Salahub, D. R. *Chem. Phys. Lett.* **1990**, *169*, 387.
(13) Duarte, H. A.; Salahub, D. R.; Haslett, T.; Moskovits, M. *Inorg. Chem.* **1999**, *38*, 3895.
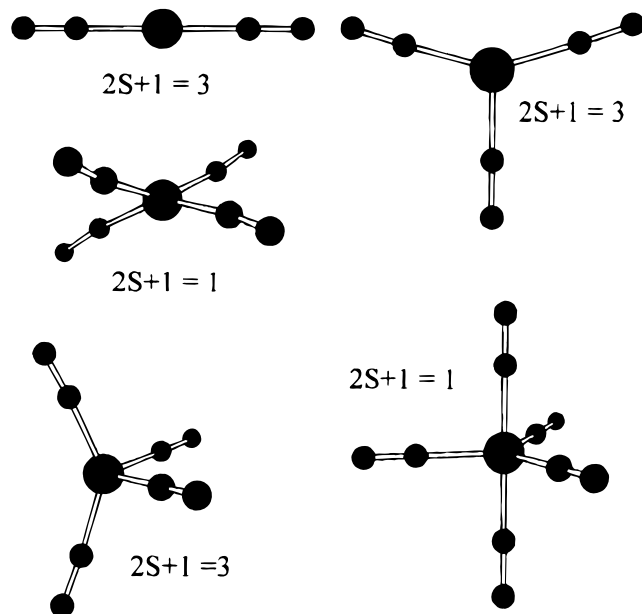(14) Becke, A. D. *Phys. Rev. A* **1988**, *38*, 3098.
(15) (a) Perdew, J. P. *Phys. Rev. B* **1986**, *33*, 8822. (b) Perdew, J. P. *Phys. Rev. B* **1986**, *34*, 7406.
(16) (a) Godbout, N.; Salahub, D. R.; Andzelm, J.; Wimmer, E. *Can. J. Chem.* **1992**, *70*, 560. (b) Godbout, N., Ph.D. Thesis, Université de Montréal, 1996.
(17) See: Schegel, H. B. In *Ab Initio Methods in Quantum Chemistry*; Lawley, K. P., Ed.; Wiley: New York, 1987; Vol. I.

Synthesis of Binary Iron−Dinitrogen Compounds

J. Am. Chem. Soc., Vol. 122, No. 25, 2000 6041

Figure 2. Optimized geometries of $Fe(N_2)_x$, $x = 2-5$, calculated as described in the text and ref 13.

Table 1. Calculated Total, Relative, and Ligand Binding Energies of $Fe(N_2)_x$ Complexes of Various Spin Multiplicities

complex	$2S_Z + 1$	total energy (au)	rel energ (eV)[a]	$\bar{D}_e$ (eV)[b]	D_e (eV)[c]
$Fe(N_2)$	1	−1373.21211	0.2794	−0.2794	−0.2794
	3	−1373.23258	−0.2775	0.2775	0.2775
	5	−1373.23635	−0.3801	0.3801	0.3801
$Fe(N_2)_2$	1	−1482.84096	−1.4353	0.7177	1.0552
	3	−1482.86030	−1.9616	0.9808	1.5814
$Fe(N_2)_3$	1	−1592.44169	−2.3850	0.7950	0.4234
	3	−1592.47108	−3.1847	1.0616	1.2231
$Fe(N_2)_4$	1	−1702.05764	−3.7487	0.9372	0.5641
	3	−1702.06426	−3.9289	0.9822	0.7442
$Fe(N_2)_5$	1	−1811.64769	−4.4077	0.8815	0.4789
N_2	1	−109.56583			
Fe	5	−1263.65655			

[a] Energy of the $Fe(N_2)_x$ complex relative to $Fe + xN_2$. [b] Mean binding energy, calculated as the relative energy divided by x. [c] Energy required to dissociate one ligand from the complex.

of various spin multiplicities. Clearly, the stability of the complex increases monotonically with the number of ligands, while the binding energy per ligand is a maximum for $Fe(N_2)_3$.

The binding energies reported are with respect to singlet N_2 and the quintet ground state of Fe. The calculation for Fe relaxing all symmetry and configuration restrictions yields a $d^{6.412}s^{1.587}$ Mulliken population, which is close to the d^6s^2 ground state. Basis set superposition error, estimated to be less than 0.03 eV for complete dissociation of $Fe(N_2)_5$, was ignored.

To predict IR spectra from the DFT calculations, the Hessian matrix was evaluated numerically to extract the harmonic vibrational frequencies of the most stable species and their $^{15}N_2$ isotopomers. This calculation also served to confirm that all structures reported were minima on the potential energy surfaces since all the calculated frequencies were real. The calculated frequencies and IR intensities for all combinations of $^{15}N_2$ isotopically substituted $Fe(N_2)_5$ are shown in Table 2. Note that we consider only the vibrations of the N_2 ligands as these are the only ones accessible in the IR experiment (the MCT detector used has a low-frequency cutoff of 900 cm^{-1}). Similar data were also calculated for both low-lying geometries of $Fe(N_2)_4$.

Results

$Fe^+ + N_2$. The spectrum obtained from a deposit of Fe^+ in N_2 is shown in Figure 3A. Three strong peaks at 2095, 2078,

and 2071 cm^{-1} dominate the spectrum, with numerous weaker peaks at 2219, 2157, 2147, 2087, 2051, 2043, 1997, 1983, 1961, 1955, 1943, and 1930 cm^{-1}. Other weak peaks above 2100 cm^{-1} do not profile and are assigned to unknown matrix impurities. Interestingly, the spectrum is more intense than that due to $Fe(CO)_5$ when normalized to the amount of Fe deposited.

The spectrum of a deposit in $^{15}N_2$ (Figure 3B) is virtually identical with a constant decrease in vibrational frequencies by a factor of 1.034, as compared to an expected value of 1.035 for a purely harmonic N_2 oscillator. A matrix formed from a mixture of $^{14}N_2$ and $^{15}N_2$ (approximately 1.5:1) yields a spectrum wherein the frequencies of the most intense peaks are different than for either pure isotopic deposit and a number of intermediate peaks are observed as well as numerous weak peaks (Figure 3C).

Deposits were also done using a higher electron flux than usual and no electrons at all. The maximum IR signal was observed for the intermediate electron flux, with a small decrease on increasing the electron flux and a large decrease when no reneutralization electrons were introduced. Annealing of the $^{14}N_2$ matrix produced no significant change in the relative peak intensities, while the absolute intensity of the spectrum gradually decreased as the matrix evaporated.

$Fe_2^+ + N_2$. On depositing Fe_2^+ in N_2, the spectrum is complicated, having peaks at 2261, 2252, 2220, 2185, 2173, 2162, 2148, 2139, 2121, 2086, 2037, 2029, 2022, 2017, 2012, and 1778 cm^{-1} (Figure 4). The intensity of the peak at 1917 cm^{-1} does not vary across the deposit like the rest of the spectrum and is assigned to an unknown matrix impurity. Also observed are the three intense peaks seen in the spectrum of the monomer deposit. The spectrum corresponds well to earlier spectra,[5,8,9] the main difference being the absence of the two peaks at 2016 and 2111 due to an $Fe(N_2)_y$ complex. As in the case of the monomer deposit, the spectrum experiences no change in relative intensities of the peaks on annealing the matrix.

$Fe_3^+ + N_2$. The IR spectrum observed on depositing Fe_3^+ with N_2 is less complex than the Fe_2/N_2 spectrum, with peaks at 2288, 2226, 2221, 2212, 2195, 2176, 2161, 2146, 2138, 2122, 2095, 2076, 2059, 2050, 2034, and 1969 cm^{-1}. As shown in Figure 5, the spectrum changes on annealing, with peaks at 2212, 2122, and 2059 cm^{-1} increasing only slightly in intensity on annealing, peaks at 2226, 2221, 2095, and 2050 cm^{-1} decreasing slightly, and peaks at 2176, 2146, and 2138 cm^{-1} decreasing strongly. Only very weak peaks are observed corresponding to the peak positions observed from the Fe^+/N_2 deposit.

Discussion

**$Fe^+ + N_2$.** Of all previously reported spectra of Fe/N_2 reaction products, the only strong resemblance to the observed spectrum is that of Chertihin et al.,[10] which is perhaps not surprising in that those experiments most closely parallel the relatively energetic cationic deposit reported here. Although we observe fewer peaks, particularly in the region from 2100 to 2200 cm^{-1}, this also is reasonable since we deposit only the Fe^+ and N_2 while the laser vaporization experiments produce both charged species of Fe in addition to neutrals and charged and dissociated nitrogen species. The three strong peaks are assigned to the same species $Fe(N_2)_x$ on the basis of the constant relative intensities observed under a number of deposition conditions and annealing. Furthermore, the same characteristic spectrum was observed from deposits of Fe_2 due to fragmentation of the dimer on deposition. This then restricts x to a value of at least 3 and at most 5, assuming the complex would be saturated at that point.

From very dilute matrix isolation of evaporated Fe in N_2,[7,8] there is also clearly a second stable $Fe(N_2)_y$ complex showing

Table 2. Calculated Frequencies (in cm^{-1}) of Isotopically Substituted Fe(^{15}N$_2$)$_{x+y}$(^{14}N$_2$)$_{(3-x)+(2-y)}$ Molecules[a]

xy	a$_2'$	e$'$		a$_1'$	a$_1'$
00	2156.6 (6.3)	2128.7 (40.2)	2126.1 (21.3)	2216.5 (3.9)	2135.1 (1.0)
01	2085.8 (4.2)	2129.0 (37.9)	2126.2 (20.3)	2205.7 (5.0)	2143.1 (5.1)
02	2083.6 (5.9)	2129.0 (36.8)	2126.2 (20.0)	2187.9 (7.2)	2089.7 (2.5)
10	2156.6 (6.4)	2126.2 (19.1)	2064.9 (15.3)	2210.5 (7.2)	2132.3 (24.2)
11	2089.6 (12.8)	2126.3 (18.9)	2062.3 (11.3)	2198.8 (9.6)	2140.2 (19.2)
12	2083.6 (6.0)	2126.3 (18.9)	2060.8 (9.6)	2177.3 (19.4)	2095.9 (17.7)
20	2156.6 (6.4)	2071.4 (5.8)	2056.7 (31.3)	2204.4 (4.2)	2129.0 (22.6)
21	2096.0 (9.8)	2135.4 (19.2)	2056.6 (31.7)	2192.1 (5.9)	2064.7 (3.4)
22	2083.7 (5.9)	2062.0 (2.4)	2056.5 (32.0)	2164.3 (15.2)	2105.0 (14.3)
30	2156.6 (6.4)	2056.9 (35.7)	2054.3 (19.5)	2198.3 (1.2)	2079.8 (5.9)
31	2109.4 (6.7)	2056.9 (36.7)	2054.2 (19.5)	2185.4 (2.4)	2066.7 (2.8)
32	2083.7 (6.0)	2056.8 (37.5)	2054.2 (19.5)	2141.6 (3.6)	2062.9 (0.9)

[a] Here, x is the number of equatorial and y the number of axial ^{15}N$_2$ ligands, the remaining being ^{14}N$_2$. Note the symmetry assignments are strictly valid only for the D_{3h} molecules ($xy = 00, 02, 30,$ and 32). Infrared Intensities in Km mol^{-1} are given in parentheses.
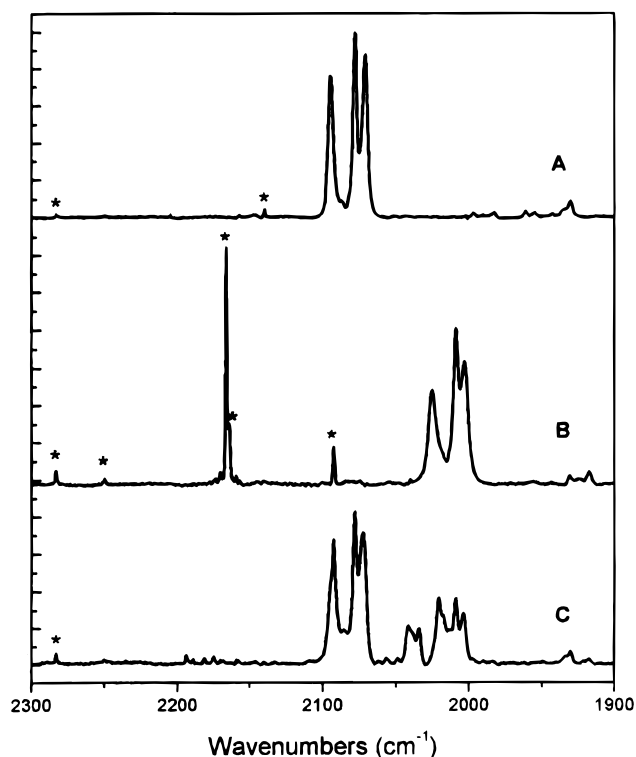
Figure 3. FTIR spectrum of Fe$^+$ (7.9 × 10^{14} in a 3 mm^2 spot) co-deposited with N$_2$ at a dilution of 10^4: (A) ^{14}N$_2$; (B) ^{15}N$_2$; (C) ^{14}N$_2$: ^{15}N$_2$ 1.5:1. The absorbance intensity of the 2078 cm^{-1} band in spectrum A is 5 × 10^{-2}. A broad baseline due to interference of the matrix has been subtracted in each case.

Figure 4. FTIR spectrum of Fe$_2^+$ (2.3 × 10^{14} in a 3 mm^2 spot) co-deposited with N$_2$ at a dilution of 10^4. The absorbance intensity of the 2078 cm^{-1} band is 3.5 × 10^{-2}. A broad baseline due to interference of the matrix has been subtracted.

two peaks at 2016 and 2111 (Figure 1A). In this complex, y is very likely greater than 2 since all previous reports have assigned other peaks to FeN$_2$ and Fe(N$_2$)$_2$ complexes.[7-10] Further assuming that more energetic deposition conditions will produce a more saturated complex implies that $x > y$. This assumption is reasonable, especially when considering the initial step of the reaction, i.e., Fe + N$_2$ → FeN$_2$. The neutral ground-state configuration of 4s^{2}3d^5 is less reactive than an excited state having a 4s^{1}3d^6 configuration, with the promotion energy to an open s-shell being a barrier in transition metal reactions as exemplified by the reaction of Mo with N$_2$.[18] The cation ground state has a configuration of 4s^{1}3d^5, thus removing the significant barrier experienced by the neutral atom. This is very likely the reason that atomic iron dinitrogen complexes have been difficult to synthesize and characterize using evaporative matrix techniques.

In contrast, with cationic atom deposition the reaction is extremely facile and complete. This results in the strong spectrum observed relative to Fe(CO)$_5$ and the weaker spectra previously attributed to Fe(N$_2$)$_x$ complexes.[7,8] The drop in signal when using a higher electron flux during deposition can also be understood since the higher electron flux should neutralize a higher proportion of the ion beam before reaction with N$_2$ occurs. Hence the conditions of deposition and the metal concentration in the matrix play a major role in the distribution of complexes formed and account for the myriad of seemingly incongruent results reported for Fe/N$_2$ deposits.

A comparison of the spectrum of Figure 3A to the known spectrum of Fe(CO)$_5$ shows an uncanny resemblance. For the carbonyl complex, the three observed peaks are assigned to the A$_2$ mode and the E mode, split in a pure CO matrix by 6 cm^{-1}.[11]

On the basis of the above discussion, the three main peaks in the spectrum are assigned to a D_{3h} end-on Fe(N$_2$)$_5$ complex analogous to Fe(CO)$_5$. The line at 2095 cm^{-1} is assigned to the A$_2$ vibration, while the lines at 2078 and 2071 cm^{-1} are assigned to an E mode, split due to a lowering of the symmetry when the complex is trapped in an N$_2$ matrix. End-on bonding is normally much more favorable and is likely the case here in that side-bound N$_2$ should have a vibrational frequency on the order of 300 cm^{-1} lower.[9,10,13]

This assignment is further strengthened by a comparison of the spectrum of the mixed ^{14}N$_2$/^{15}N$_2$ matrix to the results of

(18) Foosnaes, T.; Pellin, M. J.; Gruen, D. M. *J. Chem. Phys.* **1983**, *78*, 2889.
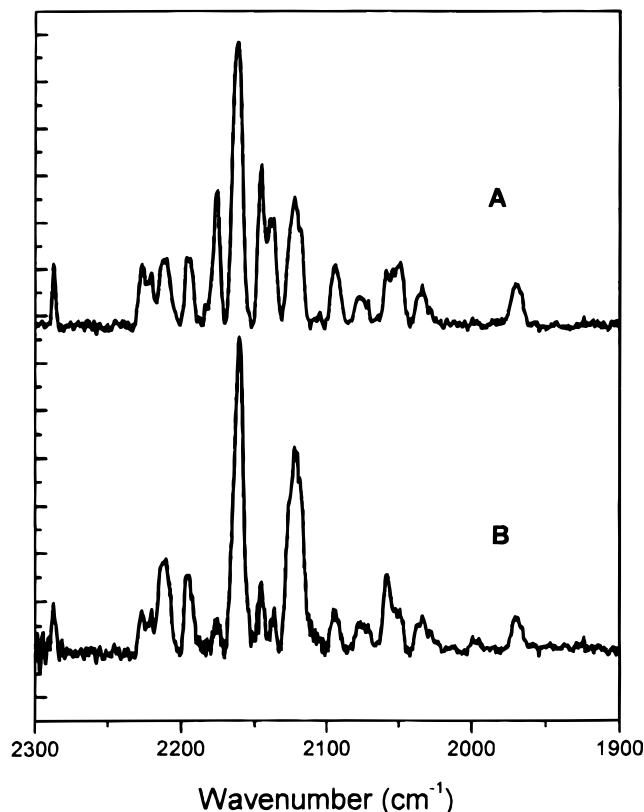
**Figure 5.** FTIR spectrum of Fe_2^+ (1.4×10^{14} in a 3 mm^2 spot) co-deposited with N_2 at a dilution of 10^4: (A) on deposition and (B) after annealing. The absorbance intensity of the 2161 cm^{-1} band is 1.2×10^{-2}. A broad baseline due to interference of the matrix has been subtracted.

Figure 6. Best fit spectra from a normal-mode analysis of a combination of isotopically substituted complexes of (A) $Fe(N_2)_4$ and (B) $Fe(N_2)_5$, calculated for the experimental ratio of 1.5:1 $^{14}N_2$:$^{15}N_2$. The measured spectrum is shown (dashed line) for comparison.

DFT calculations and to fits using a vibrational analysis based on a Cotton−Kraihanzel approach[19] as described below.

To simulate the mixed isotope matrix spectrum for $Fe(N_2)_5$ from the DFT calculations, the vibrational analysis results from Table 2 were summed with appropriate statistical weighting for each isotopic species. A similar procedure was followed to simulate the $Fe(N_2)_4$ isotopic spectrum from DFT results. Although neither calculated spectrum matches the observed spectrum very well, the general pattern of peaks is better matched by the pentadinitrogen complex, in particular with regard to the higher frequency weaker peaks. Both energetically and from vibrational frequencies, the DFT results confirm that the ligands are end-bound to the metal atom. In addition to the frequency calculations, it is interesting to note that the DFT results also predict the observed stronger IR absorption of $Fe(N_2)_5$ as compared to $Fe(CO)_5$ (see Table 7 of ref 13).

In addition to the DFT vibrational analysis, a Cotton−Kraihanzel approach was employed, wherein we assume that in the complex the N_2 ligand vibrations are not coupled to Fe−N vibrations and the two frequency regimes can then be considered separately. The Wilson GF matrix method is then applied to solve for the frequencies and intensities of the IR spectrum in the ligand region. In an iterative process, best fit spectra can then be obtained for a given assumed force field.

Since we require a minimum of 3 dinitrogen ligands to account for the observed spectrum, we first consider the complex $Fe(N_2)_3$. This possibility can be rejected in that although 3 frequencies are expected, at most two should have significant
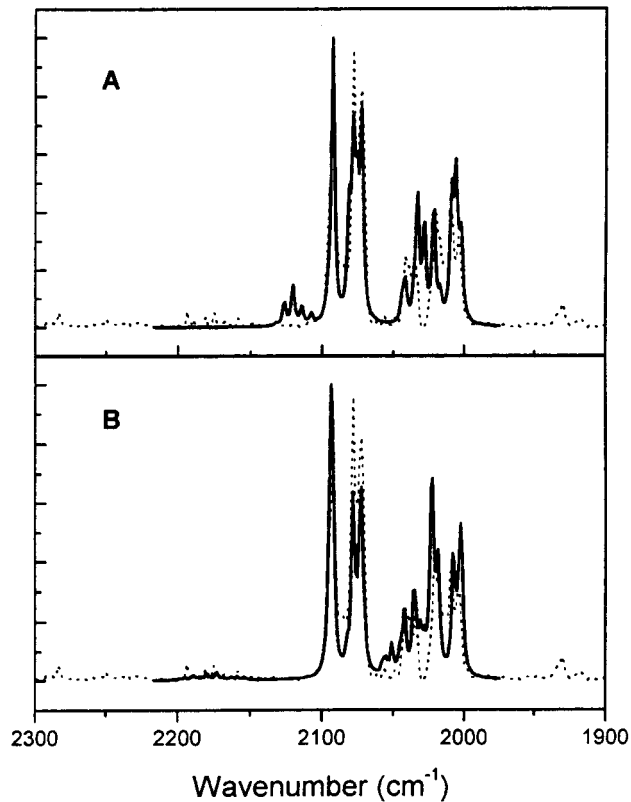
(19) Haas, H.; Sheline, R. K. *J. Chem. Phys.* **1967**, *47*, 2996 and references therein.

intensity. We thus focus our attention on the tetra- and pentadinitrogen complexes.

The D_{2d} geometry of $Fe(N_2)_4$ calculated by DFT was used, with two primary force constants and three distinct interaction constants. For $Fe(N_2)_5$, the geometry used was trigonal bipyramidal. (It is useful to note that since we consider only the ligand vibrations, the actual geometry is much less critical than is usually the case in normal coordinate analysis. To a large extent, only the symmetry of the complex is important in determining the unique force constants.) To allow for the splitting of the E mode, three primary force constants were used: one for the axial ligands, one for a unique equatorial ligand, and one for the remaining equatorial ligands. The five interaction constants between them were also included. Given a force constant matrix for the complex, the vibrational frequencies and intensities were calculated for all possible isotopically substituted $^{14}N_2/^{15}N_2$ complexes having the same structure. The isotopic spectra were then combined with appropriate statistical weighting to achieve an overall spectrum. Using a standard minimization routine (MathCAD software) with all unique force constants as variables, the calculated spectrum was fit to the experimental spectrum (Figure 3C). The results are shown in Figure 6. Although the calculated spectrum of the pentadinitrogen complex produces a better fit, the difference is not striking at first glance. However, some small details provide important evidence for the assignment.

For example, using the same parameters from the fit and comparing the spectrum observed of Fe in pure $^{14}N_2$ (Figure 3A) to the calculated spectrum of the appropriate complex, there is very good agreement for $Fe(N_2)_5$ while for $Fe(N_2)_4$ the best fit frequencies differ from the observed values by at least 1 cm^{-1}, leading to a noticeably worse fit.

Perhaps more importantly, when the region above 2100 cm^{-1} is considered there are a number of peaks with nonzero intensity expected for a tetradinitrogen complex where none are observed, while the pentadinitrogen complex predicts weak peaks in a higher frequency region where such peaks are indeed present in the spectrum. In fact, the peak observed just above 2200 cm^{-1} in Figure 3A is accounted for in this fit. The peaks above 2100 cm^{-1} are not accounted for but all have also been observed by Chertihin et al.[10] and are assigned to unknown Fe/N$_2$ complexes. With the exception of the band at 1930 cm^{-1}, Chertihin et al.[10] did not report any of the same peaks below 2070 cm^{-1}, whereas the peaks at 1997 and 1982 cm^{-1} are seen in the earlier work shown in Figure 1.[8] Although the frequencies are higher than expected for side-bonded N$_2$, these peaks may be due to complexes with a mixture of side and end-bonded N$_2$ ligands, or perhaps unsaturated end-bound complexes.

Taken together, the evidence from the DFT and Cotton–Kraihanzel vibrational analyses strongly points to Fe(N$_2$)$_5$ as the species responsible for the spectrum observed on co-depositing Fe$^+$ and N$_2$. The stable complex observed previously[7,8] is then assigned as Fe(N$_2$)$_3$ or Fe(N$_2$)$_4$. Here the assumption is that there are energy barriers to successive additions of ligand and the more energetic deposition is required to take the reaction to completion.

While Chertihin et al.[10] report the 2071 and 2078 cm^{-1} to be due to Fe(N$_2$)$_2$, this assignment does not take into account the equally strong 2095 cm^{-1} band they also report that is assigned to an unknown Fe(N$_2$)$_x$ species. Furthermore, the isotopic spectra on which the assignment is largely based are complicated by the presence of multiple species in the matrix, making deconvolution of the spectrum into component spectra attributable to particular species difficult. Thus the assignment of Fe(N$_2$)$_2$ in ref 10 is less well-supported than most of the assignments made in that in-depth study. The consistent body of evidence described above, particularly the stability of the relative intensity of the three strongest peaks under a wide range of deposition, isotopic, and annealing experiments, suggests that the three strong peaks are indeed due to a single species. This result demonstrates the advantage of depositing a mass-selected cluster beam to form the matrix, thus simplifying the spectra and assignments.

Fe$_2$$^+$ + N$_2$. Unlike the atomic deposits discussed above, the major binary complexes formed by Fe$_2$ and N$_2$ are the same regardless of the method of reaction. This is made clear by the strong similarities between the spectra from Fe$_2$$^+$ deposited directly (Figure 4) with previously reported matrix isolation work (Figure 1C).[5,8,9] All major differences can be attributed to the presence of different atomic species in the two spectra. The intensity of the Fe(N$_2$)$_5$ spectrum in Figure 4 is consistent with the 25–30% fragmentation observed on depositing Fe$_2$ in CO matrices.[11] The consistent relative intensity of the three peaks assigned to Fe(N$_2$)$_5$ as compared to Figure 3 also confirms the monomer complex assignment. Note the band at 2139 cm^{-1} is comprised of two components, with the broader assigned to an Fe$_2$(N$_2$)$_x$ complex and the sharper assigned to a small amount of CO impurity in the matrix.

While annealing experiments showed a decrease in the entire spectrum, this was most likely due to the very thin matrix evaporating in the vacuum. Annealing studies done on much thicker matrices by Mascetti and Elustondo[9] indicate that at least the major peaks in the manifold near 2017 cm^{-1} are due to a different species than the bands above 2100 cm^{-1} since they decrease in favor of the higher frequency bands on annealing. They assign those peaks to Fe$_2$(N$_2$)$_2$ based on the annealing behavior and DFT calculations. In the same work, a doublet at

1772 cm^{-1}, corresponding to the peak we observe at 1778 cm^{-1}, is assigned to side-bound Fe$_2$(N$_2$)$_2$ on the basis of observation in pure N$_2$, mixed isotope, and mixed Ar/N$_2$ (>10% N$_2$) matrices. The assignment is reasonable since the frequency is in the expected region for side-bound N$_2$ and we observe the peak only in the dimer and not the atom deposit.

Given the impossibility of performing isotopic studies and the inconclusive annealing results due to the extremely thin and dilute matrices formed in these experiments, the remainder of the peaks can only be assigned to one or more unknown Fe$_2$(N$_2$)$_x$ complexes.

Fe$_3$$^+$ + N$_2$. On inspection of the spectrum of the Fe$_3$$^+$ deposit (Figure 5), it seems that little fragmentation has occurred given the absence of significant peaks corresponding to Fe(N$_2$)$_x$ species. This includes not only the Fe(N$_2$)$_5$ peaks assigned above, but also peaks in the range 2000–2050 cm^{-1}, where all previously assigned atomic complexes appear.[7–10] Furthermore, the absence of relatively strong peaks at 2252, 2185, 2086, 2017, and 2012 cm^{-1} appearing in the spectrum of the Fe$_2$$^+$ deposit (Figure 4) suggests that little or no dimer complexes have been formed. While this lack of fragmentation is possible, it is somewhat surprising given the fragmentation observed on depositing Fe$_3$$^+$ in CO and Ar.[11,20] It is certainly possible that the trimer fragments to Fe$_2$$^+$ and Fe, where the Fe may be very unreactive, as discussed previously, and the dimer fragment forms only one of the number of complexes responsible for the spectrum of Figure 4. All peaks from 2121 to 2173 cm^{-1} are either present in the trimer spectrum or obscured by intense peaks. The peaks at 2095 and 2076 cm^{-1} could be partially due to Fe(N$_2$)$_5$ from fragmentation of the trimer.

Over a period of days, even without annealing, it was clear that the spectrum changed. The almost complete disappearance of peaks at 2176, 2146, and 2138 cm^{-1} could indicate the presence of unsaturated Fe$_3$(N$_2$)$_x$ complexes that slowly react with the matrix or a slow annealing of matrix sites. In either case, the same result is observed at an accelerated pace on gentle annealing of the matrix.

Again, experimental difficulties preclude isotopic studies, precluding a structural assignment in the absence of other evidence.

Conclusion

A series of Fe$_x$(N$_2$)$_y$ complexes have been synthesized by co-depositing the appropriate mass-selected cluster with excess N$_2$. Detailed isotopic studies and normal-mode analysis of the IR spectra, coupled with DFT calculations, lead to the assignment of end-bound Fe(N$_2$)$_5$ as the dominant atomic complex, analogous to the isoelectronic Fe(CO)$_5$. The spectrum of Fe(N$_2$)$_5$ in the matrix shows that the symmetry is lowered from the ideal D_{3h} trigonal-bipyramidal structure, similar to the result observed for Fe(CO)$_5$. DFT calculations along with the Fe(CO)$_5$ analogue suggest that the gas-phase structure may well have the D_{3h} structure. FTIR spectra attributed to one or more Fe$_2$(N$_2$)$_x$ complexes and one or more Fe$_3$(N$_2$)$_y$ complexes are also reported. Since isotopic studies were not possible for the Fe$_2$ and Fe$_3$ experiments, no structures for these complexes have been assigned.

(20) Haslett, T. L.; Bosnick, K. A.; Fedrigo, S.; Moskovits, M. *J. Chem. Phys.* **1999**, *111*, 6456.